within a wedge of tens of milliradians. Thus, powder electron data generally tend to be more kinematical than single-crystal data.

2.4.3. Electron powder diffraction techniques

By J.-M. Zuo and J. Zhang

The basic setup for electron powder diffraction uses a transmission electron microscope equipped with an area electron detector (photographic film, CCD camera *etc.*). Thin films, such as amorphous carbon or holey carbon films supported on metal grids, are typically used to support powder samples, which are then mounted and inserted into the transmission electron microscope inside a TEM sample holder. Solid free-standing thin films can be placed directly on top of a metal grid.

The electron beam used for a powder electron diffraction experiment is shaped using electromagnetic lenses. A modern transmission electron microscope uses at least three sets of magnetic lenses for the illumination system: condensers I and II, and the objective prefield. The prefield is part of the objective lens system before the sample acting as a lens. Some transmission electron microscopes come with an additional condenser lens (condenser III, or condenser mini-lens), which can be used for nanodiffraction. These lenses are used in various combinations to set up electron illumination for selected-area electron diffraction (SAED) or nano-area electron diffraction (NAED) (Zuo, 2004). The major difference between these two is the area of illumination, which is controlled by the strength (or focal length) of the condensers II and III.

An issue to be considered during setup of the electron beam for powder diffraction is the electron lateral coherence length. In a transmission electron microscope, the electron coherence is defined by the coherence length seen at the condenser aperture. According to the Zernike–Van Cittert theorem, the degree of coherence between electron wavefunctions at two different points far away from a monochromatic electron source is given by the Fourier transform of the source intensity distribution (Cowley, 1999). If we assume that the source has a uniform intensity within a circular disc, the coherence function is then given by $\lambda J_1(\pi\beta r/\lambda)/\beta r$ with J_1 being the first-order Bessel function, r the radial distance at the aperture and β the angle sustained by the electron source. The lateral coherence length L, which is often referred to in the literature, is defined by r at the first zero of J_1, which has the value of $L = 1.2\lambda/\beta$. The source seen by the condenser aperture inside a transmission electron microscope is the source image formed after the condenser-I lens. For a Schottky emission source, the emission diameter is between 20 and 30 nm according to Botton (2007). For a condenser aperture placed 10 cm away from the electron source image, a factor of 10 source demagnification provides a coherence length from 100 to 150 µm. When a smaller condenser aperture is used, such as in NAED, the electron beam can be considered as approximately coherent and the lateral coherence length on the same is limited by the beam convergence angle α with $L_{\text{sample}} = 1.2\lambda/\alpha$.

2.4.3.1. *Selected-area electron diffraction (SAED)*

SAED is formed using the transmission electron microscope illumination, which is spread out over a large area of the specimen to minimize the beam convergence angle. The diffraction pattern is first formed at the back focal plane of the objective lens and then magnified by the intermediate and projector lenses

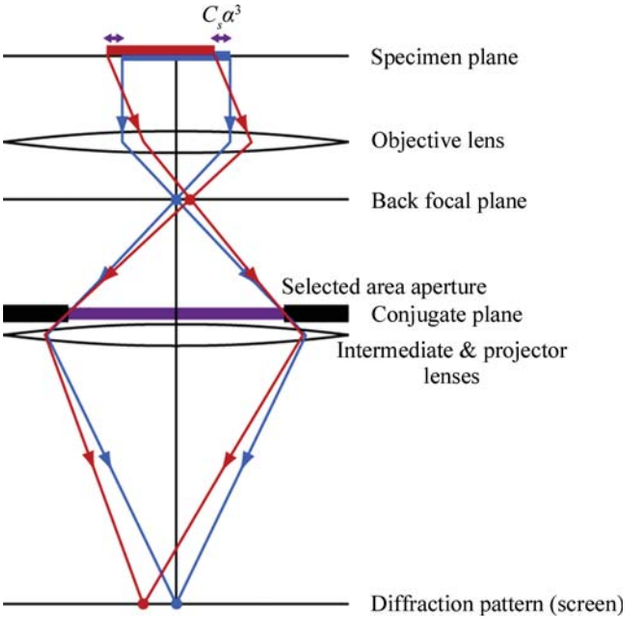

Figure 2.4.3
Schematic illustration of selected-area electron diffraction in conventional TEM. (Provided by Jun Yamasaki of Nagoya University, Japan.)

(only one is shown) onto the screen or electron detector (Fig. 2.4.3). The recorded diffraction pattern is from an area of interest selected by placing an aperture in the conjugate (imaging) plane of the objective lens. Only electron beams passing through this aperture contribute to the diffraction pattern. For a perfect lens without aberrations, electron beams recorded in the diffraction pattern come from an area that is defined by the image of the selected-area aperture at the specimen plane. The aperture image is demagnified by the objective lens. In a conventional electron microscope, rays at an angle to the optic axis are displaced away from the centre because of the spherical aberration of the objective lens (C_s) as shown in Fig. 2.4.3. The displacement is proportional to $C_s\alpha^3$, where α is twice the Bragg angle. The smallest area that can be selected in SAED is thus limited by the objective lens aberrations. This limitation is removed by using an electron microscope equipped with a transmission electron microscope aberration corrector placed after the objective lens (Haider *et al.*, 1998).

The major feature of SAED is that it provides a large illumination area, which is beneficial for recording diffraction patterns from polycrystalline samples as it leads to averaging over a large volume (for example, a large number of nanoparticles). SAED can also be used for low-dose electron diffraction, which is required for studying radiation-sensitive materials such as organic thin films.

2.4.3.2. *Nano-area electron diffraction (NAED)*

NAED uses a small (nanometre-sized) parallel illumination with the condenser/objective setup shown in Fig. 2.4.4 (Zuo *et al.*, 2004). The small beam is achieved by reducing the convergence angle of the condenser-II crossover and placing it at the focal plane of the objective prefield, which then forms a parallel-beam illumination on the sample for an ideal lens. A third condenser lens, or a mini-lens, is required for the formation of a nanometre-sized parallel beam. For a condenser aperture of 10 µm in diameter, the probe diameter is ∼50 nm with an overall magnification factor of 1/200 in the JEOL 2010 electron microscopes (JEOL, USA). The smallest beam convergence angle in NAED is

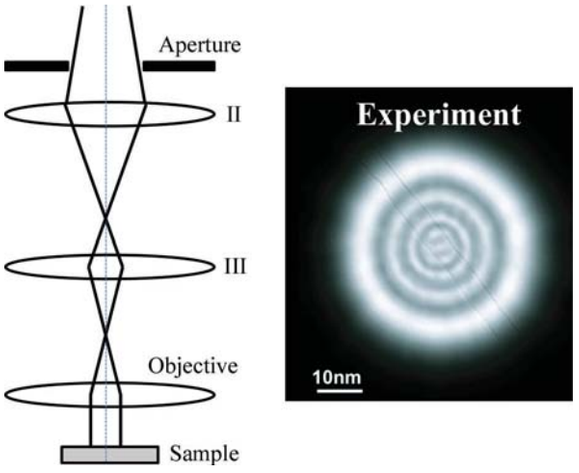

Figure 2.4.4
Schematic illustration of electron nanoprobe formation using a combination of condenser lenses (II and III) and the objective lens. The beam divergence angle is kept at a minimum by forming a crossover at the front focal plane of the objective lens. An image of an experimental electron nanoprobe is shown on the right with a carbon nanotube contained inside the probe.

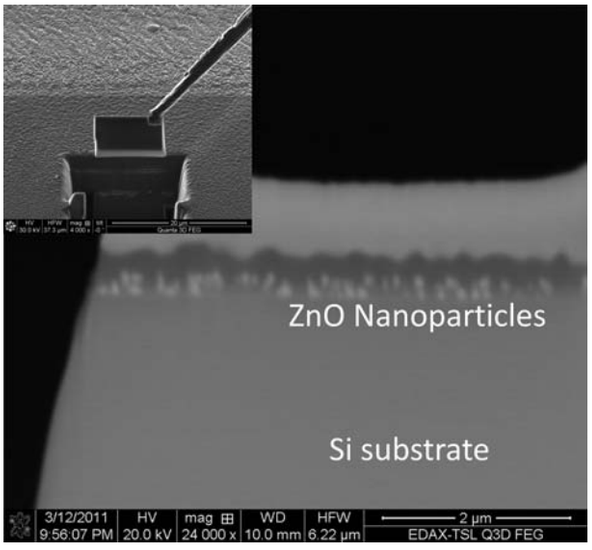

Figure 2.4.5
Sample preparation and lift-out using a focused ion beam (FIB). A thin section of the sample is cut out using the FIB and attached to a mechanical probe for lift-out (inset). The image shows the lift-out section containing ZnO nanoparticles in bright dot-like contrast supported on an Si substrate.

limited by the aberrations of the illumination lenses. A beam convergence angle as small as ∼0.05 mrad has been reported (Zuo *et al.*, 2004). A diffraction pattern recorded using NAED is similar to one recorded by SAED. The major difference is that the diffraction volume is defined directly by the electron probe in NAED. Since all electrons illuminating the sample are recorded in the diffraction pattern, NAED in an FEG microscope also provides higher beam intensity than SAED (the probe current intensity using a 10 µm condenser-II aperture in a JEOL 2010F is $\sim 10^5$ e s^{-1} nm^{-2}) (Zuo *et al.*, 2004).

The small probe size is most useful for studying a small section of thin films or for selection of nanoparticles for powder diffraction. The small beam size reduces the background in the electron diffraction pattern from the surrounding materials.

2.4.3.3. *Sample preparation*

The success of an electron powder diffraction experiment to a large extent depends on sample preparation. The powder sample has to be suitable for electron-beam observation, and the sample also needs to be compatible with the vacuum environment of the microscope. *In situ* experiments can be carried out using special holders for cooling, heating and cryogenic or environmental transfer. Special microscopes are also available to provide a gaseous or ultra high vacuum environment for the investigation of structures under a gas or at ultra low pressure, or *in situ* sample preparation.

The observed area of the sample must be electron transparent, *i.e.* have a thickness of less than or comparable to the inelastic mean free path of electrons. The inelastic mean free path increases with the electron voltage (Egerton, 2011). The typical sample thickness ranges from a few tens to hundreds of nanometres for 200 kV high-energy electrons (see Table F.1 in Zuo & Spence, 2017).

The sample-preparation techniques can be divided into three categories: (i) bulk-based for bulky materials and supported thin films, (ii) powder-based techniques and (iii) free-standing thin films over a supporting grid prepared by vacuum evaporation or sputtering.

The bulk-based techniques involve mechanical cutting, thinning/polishing and perforation. An ion beam is typically used in the last step of perforation to create a thin area around the edge of a hole for electron-beam observation. Chemical and electrolytic methods are also often used for preparing electron-transparent samples. While these methods have been applied to a broad range of materials, they are mostly used for metals or semiconductors to create smooth sample surfaces free from defects or sample heating caused by ion-beam irradiation. Mechanical thinning and polishing are sometimes done with a wedge angle with the help of a tripod. The thin region next to the edge only requires a brief ion-beam bombardment to make it electron transparent. A detailed description of traditional sample-preparation techniques for TEM can be found in Barna & Pécz (1997). The above techniques are applicable to both thin films and bulk nanocrystalline materials. The powder-based techniques use dispersion of powders on thin supporting films placed on metal grids specially made for TEM observations. This technique is most suitable for nanoparticles. For micron or larger-sized powders, additional grinding is used to produce smaller particles. The most commonly used supporting films are continuous amorphous carbon films, holey carbon films, networked carbon fibres (lacey carbon), amorphous silicon nitride and SiO_x. For amorphous carbon films, an ultra thin version is available which is especially useful for nanoparticle samples.

A recent development in TEM sample preparation is the use of a focused ion beam of Ga^+ ions for cross-sectioning a sample. The focused ion beam can drill a precise hole in the sample. The same ion beam can also be scanned over a sample surface to form an image by collecting the secondary electrons or ions generated by the beam. The ion column can be integrated into an electron column in a scanning electron microscope in the so-called dual-beam configuration. An image can be formed using either electrons or ions. Most often the electron beam is used for sample inspection, while the ion beam is used for patterning and milling. This allows precise control over the position and thickness of the cross section, which is very practical for characterization of

semiconductor devices or failure analysis in general (Fig. 2.4.5). Further details about ion-beam techniques can be found in Lábár & Egerton (1999) and Orloff *et al.* (2002). For a comprehensive review of sample-preparation techniques for TEM, see Őzdöl *et al.* (2012).

2.4.3.4. *Diffraction data collection, processing and calibration*

Experimental electron powder diffraction data are collected using two-dimensional area electron detectors. Experimental issues involved in the diffraction-pattern recording procedure are electron optical alignment, diffraction-pattern collection and calibration, with particular care taken in adjusting the specimen height position (eucentric position), selection of a suitable illumination-beam convergence angle and diffraction-camera length, and finally projector-lens focusing. The diffraction-camera length is determined by the setting of intermediate and projector lenses in combination with the objective lens. To calibrate the diffraction-camera length, a standard sample is placed in the eucentric position of the objective lens at the standard focus. At this setting, the specimen plane is conjugate to the selected-area aperture (Fig. 2.4.3) and the sample image appears in focus. To obtain a sharp diffraction pattern, the detector plane must be conjugate to the back focal plane of the objective lens. This can be achieved by setting up a parallel-beam illumination and adjusting the intermediate-lens focus length to bring the direct beam into a sharp focus.

Currently available area electron detectors are CCD and CMOS cameras, imaging plates (IPs) and photographic film. While photographic film has a long history of use in electron microscopy, its limited dynamic range makes it less useful for electron diffraction data collection. Both CCD cameras and IPs are digital recorders capable of collecting electron intensity over a large dynamic range. The crucial characteristics of digital recording systems are the gain (g), linearity, resolution, detector quantum efficiency (DQE) and the dynamic range. The gain of a CCD or CMOS camera can be normalized using a flat-field illumination; the gain in IPs is assumed to be constant. The detector resolution is characterized by the point-spread function (PSF), which is roughly the detector's response to a point-like illumination. These characteristics for CCDs and IPs have been compared by Zuo (2000). The intensity of an electron diffraction pattern recorded with a digital detector is given by

$$I^{\text{recorded}}(i,j) = g(i,j)H(i,j) \otimes I^{\text{original}}(i,j) + n(i,j), \qquad (2.4.14)$$

where $g(i, j)$ is the detector gain image, H is the PSF of the detector, n is the detector noise and I^{original} is the intensity of scattered electron beams originally received by the detector. The i and j are the pixel coordinates of the detector. The PSF is experimentally characterized and measured by the amplitude of its Fourier transform, or the so-called modulated transfer function (MTF). The effects of the PSF can be removed by deconvolution. The Richardson–Lucy method is specifically targeted for Poisson processes, which can be applied to CCD images (Zuo, 2000). The alternative to the removal of the PSF is to treat it as part of the peak broadening that can be used to fit the powder pattern.

The noise in the experimental data is characterized by the DQE:

$$\text{var}(I) = \frac{m\bar{g}I}{\text{DQE}(I)}. \qquad (2.4.15)$$

Here I is the experimentally measured intensity, var stands for the variance, m is the area under the MTF and $\bar{g}$ is the average gain of the detector. Once the DQE is known, this expression allows an estimation of the variance in measured intensity, which is essential for quantitative intensity analysis where the variance is often used as the weight for comparing experimental and fitted data.

The performances of CCDs and IPs for electron diffraction pattern recording are different at different electron dose rates. At low dose rates, the DQE of the CCD camera is limited by the readout noise and the dark current of the CCD. IPs have better performance in the low dose range due to the low dark current and low readout noise of the photomultipliers used in IP readers. At medium and high dose rates, the IP signal is affected mostly by the linear noise due to the granular variation in the phosphor and instability in the readout system, while for CCDs the noise is mostly linear noise in the gain image.

Electromagnetic lenses are not perfect and have aberrations affecting the collected data. In most transmission electron microscopes, electron diffraction patterns are produced using the post-specimen magnetic lenses. For electron diffraction, the most important aberration is the distortion of the projector lens, causing a shift of an image point. There is no blurring in diffraction patterns associated with the lens distortion. However, the distortion affects the overall shape of diffraction patterns. The distortion is most obvious at low camera lengths, where the pattern may seem stretched or twisted at high scattering angles. There are three types of distortion of the same order as the spherical aberration of the lens. They are called pin-cushion, barrel and spiral distortions (Reimer, 1984). A distortion can also arise from the use of an electron energy filter, where a lower order of distortion can be introduced with the use of non-spherical lenses (Rose & Krahl, 1995).

For quantitative analysis an electron powder diffraction pattern recorded on an area detector needs to be integrated into one-dimensional powder diffraction data (Fig. 2.4.6). The integration involves four separate steps: (i) identifying areas of the diffraction pattern for integration, (ii) centring the diffraction pattern, (iii) applying a diffraction pattern distortion correction, if there is any, and (iv) integrating intensities for a constant diffraction angle. Electron powder diffraction patterns can be recorded on a crystalline support film, which gives sharp diffraction spots distinct from the powder diffraction rings. The sharp diffraction patterns from the support film can be excluded from the powder diffraction intensity integration in step (i) by using a mask. The same approach can be used to eliminate any alien features from a diffraction pattern caused, for instance, by the aperture or the energy filter. The diffraction pattern centring is based on the analysis of the transmitted beam in the centre of the pattern. As the transmitted beam is usually very strong and is often overexposed, finding its centre may be a non-trivial task. In order to prevent detector damage in the area of the transmitted beam a beam stop is often used. In this case, the central area in the pattern may have an irregular shape not suitable for the centring procedure. Non-distorted diffraction patterns can be centred by finding the centre of the concentric diffraction rings either by locating the position of the maximum diffraction peak intensity along the ring and using these positions to determine the centre of the ring, or by searching for the centre that gives the maximum correlation between $I(g)$ and $I(-g)$. For distorted diffraction patterns, the centring and the distortion correction must be carried out simultaneously.

The distortion correction requires a powder sample with known d-spacings. The amount of distortion can be obtained by

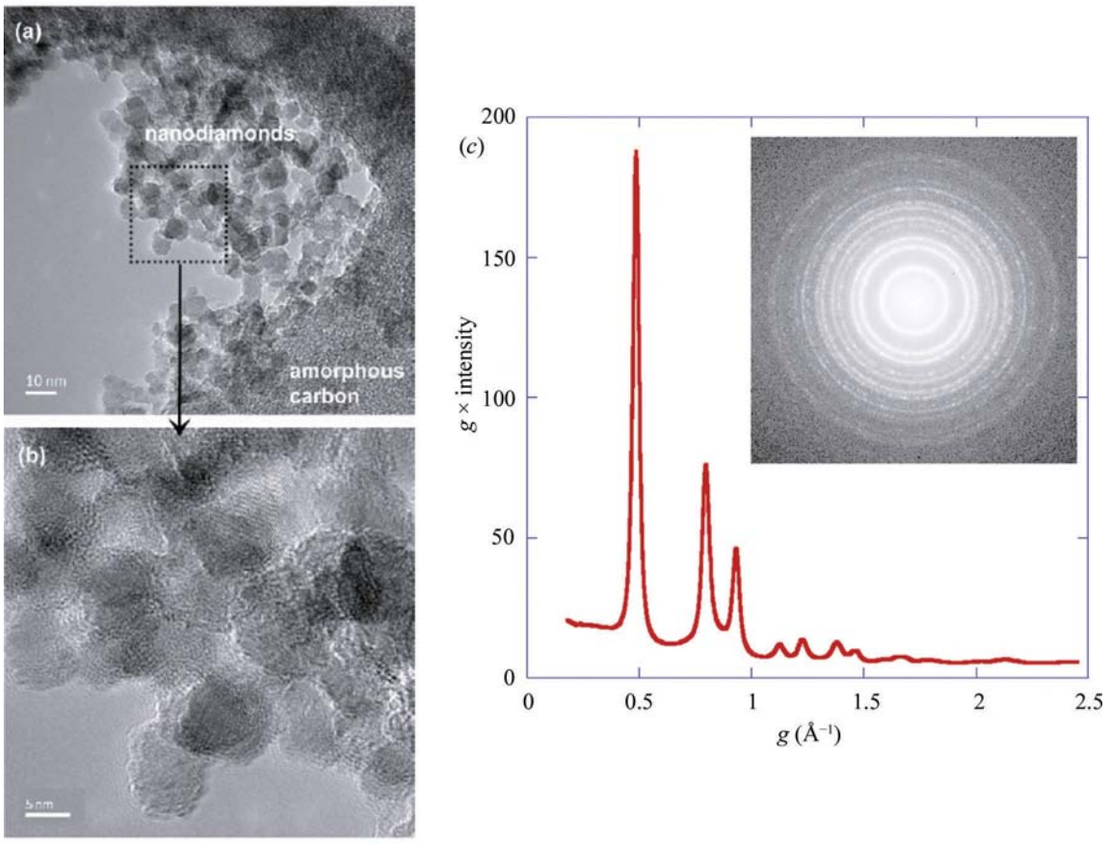

Figure 2.4.6
An example of electron powder diffraction recording for nanodiamonds. (*a*) A TEM image showing nanodiamond particles supported on amorphous carbon, (*b*) the magnified image from the boxed region of (*a*), and (*c*) the recorded electron powder diffraction pattern from nanodiamond particles and the obtained radial intensity profile.

fitting the diffraction ring position $R_d(\varphi)$ using a cosine expansion with

$$R_d(\varphi) = R + \sum_{n=1}^{N} \Delta R_n \cos n(\varphi - \varphi_n), \tag{2.4.16}$$

where R is the average radius (zero order) of the diffraction ring, ΔR represents the amplitude of distortion of order n and φ is the azimuthal angle. Once the distortion is calibrated and excluded from the data, the diffraction intensity integration can be simply carried out by summing the recorded diffraction intensity according to the radius using

$$I_n = \frac{1}{N} \sum I[i, j], \tag{2.4.17}$$

where the sum is taken over $R(i, j, i_0, j_0, \Delta R) \in \{n\delta, (n + 1)\delta\}$. Here the powder diffraction intensity is integrated in fine discrete steps along the radius of a diffraction pattern (corresponding to increasing scattering angle) with an interval of δ, the summation is done over all diffraction pixels that fall between the radius of $n\delta$ and $(n + 1)\delta$ and N is the number of these pixels.

Filtering the inelastic background is an option for electron microscopes equipped with an electron energy filter. A major contribution to the inelastic background in electron diffraction patterns comes from bulk plasmon excitation (Egerton, 2011). This can be filtered out by dispersing the electrons according to their energies using magnetic or electrostatic fields inside an electron energy filter and using a slit of a few eV in width around the elastic (zero-loss) electron beam. For use with an area electron detector for electron diffraction, the filter must also have a double focusing capability to function as an imaging lens. There are two types of electron imaging energy filters that are currently employed: one is the in-column Ω energy filter and the other is the post-column Gatan imaging filter (GIF). The in-column Ω filter is placed between the transmission electron microscope's intermediate and projector lenses and can be used in combination with IPs, as well as with a CCD or CMOS camera. The GIF is placed after the projector lens and the use of a GIF for electron diffraction typically requires the transmission electron microscope to be switched to a special low-camera-length setting. For electron diffraction, geometric distortions, isochromaticity and the angular acceptance are important characteristics of the imaging filter (Rose & Krahl, 1995). Geometrical distortions arise from the use of non-cylindrical lenses inside the energy filter. The distortion can be caused by optical misalignment, which is an issue with the GIF with its low camera-length setting. The amount of distortion can be measured using a standard calibration sample and corrected using numerical methods. Isochromaticity defines the range of electron energies for each detector position. Ideally, this should be the same across the whole detector area. The angular acceptance defines the maximum range of diffraction angles that can be recorded on the detector without a significant loss of isochromaticity (Rose & Krahl, 1995).

2.4.4. Phase identification and phase analysis

By J. L. Lábár

For known structures, powder diffraction patterns can be used for identification of the crystalline phases and quantification of their